Molecular Crystal Architecture and Optical Properties of a Thiohelicenes Series Containing 5, 7, 9, and 11 Rings Prepared via Photochemical Synthesis

Tullio Caronna,*[,†] Marinella Catellani,[‡] Silvia Luzzati,[‡] Luciana Malpezzi,[†] Stefano V. Meille,[†] Andrea Mele,[†] Christoph Richter,[§] and Roberta Sinisi[†]

Dipartimento di Chimica del Politecnico, Via Mancinelli 7, 20131 Milan, Italy, Istituto di Chimica delle Macromolecole-CNR, Via Bassini 15, 20133 Milan, Italy, and Plataforma Solar de Almeria, P.O. Box 22, 04200 Tabernas, Almeria, Spain

Received February 6, 2001. Revised Manuscript Received June 26, 2001

Helicenes are intrinsically chiral helical molecules structurally characterized by ortho-fusion of aromatic rings. A series of racemic heterohelicenes composed of thiophene and benzene rings alternated in the helical chain were prepared via photochemical irradiation. The availability of large systems containing 9 and 11 condensed rings allows a better understanding of both optical properties and solid-state organization of thiohelicene molecules. The conformation and the crystal architecture of thiohelicenes, containing up to 11 rings show ring distortions smaller than in carbohelicenes. All the crystals obtained are racemates, and heterochiral assembling is dominant also for the larger systems.

Introduction

Conjugated organic molecules have been the subject of continuous interest relating to possible applications in electronic and optoelectronic devices or as photoactive materials. Synthetic efforts aimed at π-conjugated systems having well-defined architectures are indeed driven by the desire to impart specific optical and electrical properties to materials via control of their molecular structure. In the case of helical conjugated molecules, helicity is often an essential factor that will modulate the electronic properties and influence the solid-state self-organization of such systems.

Helicenes are formed by ortho-condensed aromatic or heteroaromatic rings. The steric interactions arising in this type of condensation do not allow planarity for molecules with sequences of five or more rings and cause the π-conjugated systems to get distorted into helices which are intrinsically chiral structures.[1] Such rigid helical polyaromatics are particularly attractive because their chiroptical and electronic properties combine, yielding new effects which become more significant and reach asymptotic values increasing the molecular size. Helicenes deserve interest both as polyconjugated systems and as chiral materials. Indeed they have been investigated as helical conjugated polymers,[2] as macroscopic liquid crystalline fibers,[3] as chiral aggregates with very high specific optical rotation,[4] and also as chiral ligands in asymmetric catalysis.[5,6] The helical architecture containing a distorted conjugated system produces both intra- and intermolecular π-electron interactions that strongly influence the optical properties in solution and the molecular self-organization in the solid state. In large helicene intramolecular interactions between π-electron systems of overlapping rings, separated by one helical turn, become possible. Intermolecular stacking involving aromatic rings close to the molecular ends is a general feature of helicene packing. The organization of helicenes in the solid state is also influenced by the helical molecular geometry. In the case of nonracemic helical compounds, this molecular feature has been shown to program aggregates toward helical supramolecular architectures.[7]

The presence of heteroatoms in the helicene backbone significantly alters both the molecular and the self-assembly properties of helical polyaromatics. Thiophene and benzene rings alternate in the thiohelicenes, and thiophenes are modules expected to determine desirable effects in these systems. Indeed thiohelicenes are stable materials which can be synthesized in good yields via photochemical irradiation,[8] using either standard laboratory equipment or solar powered reactors. In this paper we report on the synthetic approach we used to prepare a series of racemic heterohelicenes: trithia[5]-heterohelicene (**TH5**), tetrathia[7]heterohelicene (**TH7**), pentathia[9]heterohelicene (**TH9**), and esathia[11]heterohelicene (**TH11**) (see Figure 1). These systems have been obtained in racemic form and were resolved by HPLC chromatography.[9−12] The improvement of the

† Dipartimento di Chimica del Politecnico.
‡ Instituto di Chimica delle Macromolecole-CNR.
§ Plataforma Solar de Almeria.

(1) Martin, R. H. *Angew. Chem., Int. Ed.* **1974,** *13,* 649 .
(2) Dai, Y.; Katz, T. J. *J. Org. Chem.* **1997**, *62*, 1274.
(3) Lovinger, A. J.; Nuckolls, C.; Katz, T. J. *J. Am. Chem. Soc.* **1998**, *120*, 264.
(4) Nuckolls, C.; Katz, T. J.; Castellanos, L. *J. Am. Chem. Soc.* **1996**, *118*, 3767.
(5) Reetz, M. T.; Beuttenmuller, E. W.; Goddard, R. *Tetraedron* **1997,** *38*, 3211.
(6) Dreher, S. D.; Katz, T. J.; Lam, K.-C.; Rheingold, A. L. *J. Org. Chem.* **2000**, *65*, 815 .
(7) Nuckolls, C.; Katz, T. J.; Katz, G.; Nuckolls, C.; Castellanos, L. *J. Am. Chem. Soc.* **1999**, *121*, 79.
(8) Groen, M. B.; Schadenberg, H.; Wynberg, H. *J. Org. Chem.* **1971**, *36*, 2797.
(9) Caronna, T.; Sinisi, R.; Catellani, M.; Malpezzi, L.; Meille, S. V.; Mele, A. *Chem. Commun.* **2000**, 1139.

10.1021/cm010093z CCC: $20.00
Published on Web 09/25/2001

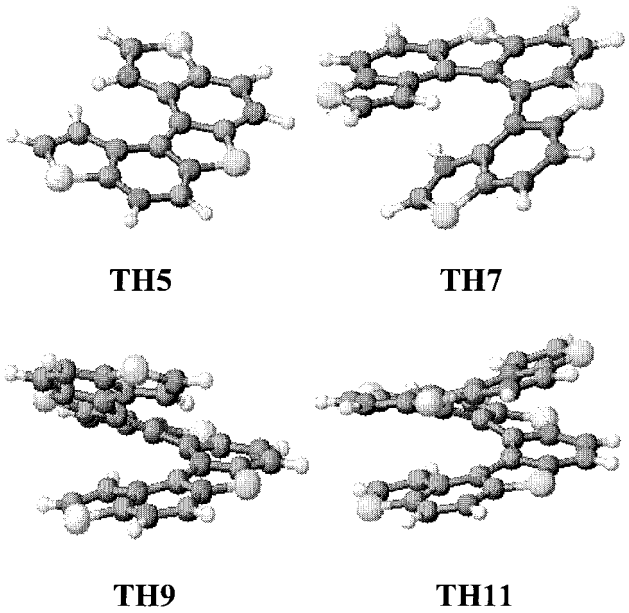

Figure 1. 5- (**TH5**), 7- (**TH7**), 9- (**TH9**), and 11-membered (**TH11**) thiohelicene.

synthetic procedure makes larger thiohelicenes available in sufficient amounts to allow a more thorough characterization. Specifically the electroluminescence properties of this molecular class may be of interest, along with the electronic spectral properties and the crystalline architecture of such helical systems, which allow one to envisage other applications. An open issue was whether the preference for heterochiral molecular aggregation shown by the racemic five-[13] and seven-member[12] thiaheterohelicenes in crystals persists also in higher members of the series, specifically with reference to the crystal structures of the two larger thiohelicenes. The determination of the crystal structure of the eleven-ring systems and the analysis of the published data pertaining to the smaller nine-, seven-, and five-ring molecules also aim at evidencing the possible role of specific interactions involving sulfur and hydrogen atoms in the crystalline organization of thiohelicenes. Indeed the presence of sulfur atoms, besides modulating the electronic properties as compared to carbohelicenes, is likely to influence significantly the self-assembly behavior of thiohelicenes.

Experimental Section

Instrumentation and Procedure. Photochemical reactions were carried out in a RPR-100 Rayonet photochemical reactor equipped with 16 F8T5/D and F8T5/CW lamps (8 W each), irradiating in the visible range (400−800 nm), or in the solar photochemical receiver/reactor "Solfin" at the Plataforma Solar de Almeria. The Solfin photochemical receiver/reactor consists of a CPC collector with aluminum reflectors and Duran glass tubes, with an optical concentration factor of 1, total aperture of 2 m^2, and an irradiated volume of up to 10 L that can be connected to a closed loop with an overall volume of 10−20 L, equipped with a gear pump, process cooler, solvent supply vessel, gas supply, and instrumentation to monitor temperature, pressure, and flow within the loop.

^{1}H NMR spectra were recorded on a Bruker ARX 400 spectrometer operating at 400 MHz and at 305 K. The samples were dissolved in C_6D_6; typical acquisition parameters are as follows: 4500 Hz spectral window, 32 k points, 10 s interscan delay. Chemical shifts are referred to internal tetramethylsilane (TMS).

Matrix assisted laser desorption/ionization time-of-flight mass spectra (MALDI-TOF-MS) were acquired on a Shimadzu-Kratos Kompact Maldi II instrument operating in the linear mode with an accelerating potential of 20 kV and equipped with a UV pulsed laser (N_2, λ = 337 nm, 100 mJ/shot, 3 ns pulse width of a single laser shot). The laser irradiance was selected manually over an arbitrary nonlinear scale ranging from 0 (null power) to 180 (full power). Once the detection threshold was reached for the interesting peaks, the irradiance was raised by 10−20%. The data were acquired with a laser irradiance within the range of 40−60 of the arbitrary scale of the instrument and by using time delayed extraction (tDE). All the spectra were acquired by scanning the sample spot along the *x* axis and averaging over 100 laser shots. The thiohelicenes showed significant absorption at the wavelength of the laser source; thus the spectra were acquired without a matrix. Preliminary tests showed similar sensitivity and resolution with and without a matrix. The data were processed on a Sun Spark 2 computer using the manufacturer software. Mass calibration was achieved using 2,5-dihydroxybenzoic acid and γ-cyclodextrin as internal references. The analytes were dissolved in spectroscopy grade dichloromethane at a typical concentration of 100 pmol/μL, corresponding to 0.1 mM. The samples were prepared by spotting 0.5 μL of analyte solution without matrix on the sample slide and allowing evaporation of the solvent under a N_2 stream.

Electronic absorption spectra of thiohelicenes were recorded with a Varian Cary 2400 spectrophotometer. The emission spectra were obtained with a Xe lamp coupled to a monochromator to select the excitation energy and a flat field spectrometer equipped with a N_2 cooled detector. The spectra were corrected for the instrumental spectral response. The emission spectra were taken on thiohelicenes dissolved in chloroform at concentrations lower than 10^{-4} M. The quantum yields of the solutions have been obtained using quinine sulfate solutions as a standard.

Crystal Data and Structure Refinement for TH9 and TH11. Data for both compounds were collected on a Siemens P4 diffractometer at room temperature, using graphite monochromated Cu Kα radiation (λ = 1.54179 Å) and $\theta/2\theta$ scans. An empirical absorption correction was applied using ψ-scan methods.

TH9. $C_{28}H_{12}S_5$, M_r =508.68, monoclinic, space group *C*2/*c* (No. 15), a = 14.655(1) Å, b = 10.656(1) Å, c = 13.976(1) Å, β = 100.25(1)°, V = 2147.7(3) Å^3, Z = 4, D_c = 1.573 g cm^{-3}, μ = 5.098 mm^{-1}, $F(000)$ = 1040; 3662 reflections (1875 unique, R_{int} = 0.078). The final refinement, for 234 refined parameters, converged to $R(F^2)$ = 0.048 (R_w = 0.123) for all unique reflections with $I > 2\sigma(I)$ after merging.

TH11. $C_{34}H_{14}S_6$, M_r = 614.81, triclinic, space group P1 (No. 1), a = 11.396(1) Å, b = 11.490(1) Å, c = 20.141(2) Å, α = 78.49(1)°, β = 89.59(1)°, γ = 88.00(1)°, V = 2582.7(4) Å^3, Z = 4, D_c = 1.581 g cm^{-3}, μ = 5.093 mm^{-1}, $F(000)$ = 1256; 9915 reflections (8582 unique, R_{int} = 0.031). The final refinement, for 806 refined parameters and 28 restraints, converged to $R(F^2)$ = 0.063 (R_w = 0.132) for all unique reflections with $I > 2\sigma(I)$ after merging.

The structures were solved by direct methods using the SIR97 program[17] and refined by full-matrix least squares with

(10) Nakagawa, H.; Ogashiwa, S.; Tanaka, H.; Yamada, K.; Kawazura, H. *Bull. Chem. Soc. Jpn.* **1981,** *54*, 1903.
(11) Yamada, K.; Ogashiwa, S.; Tanaka, H.; Nakagawa, H.; Kawazura, H. *Chem. Lett.* **1981**, 343.
(12) Nakagawa, H.; Obata, A.; Yamada, K.; Kawazura, H.; Konno, M.; Miyamae, H. *J. Chem. Soc., Perkin Trans. 2* **1985**, 1999.
(13) Nakagawa, H.; Yamada, K.; Kawazura, H.; Miyamae, H. *Acta Crystallogr.* **1984**, *C40*, 1039.
(14) Kellog, R. M.; Groen, M. B.; Wynberg, H. *J. Org. Chem.* **1967**, *32*, 3093.
(15) Larsen; Bechgaard, K. *J. Org. Chem.* **1996**, *61*, 1151.
(16) Tanaka, K.; Suzuki, H.; Osuga, H. *J. Org. Chem.* **1997**, *62*, 4465.
(17) Altomare, A.; Burla, M. C.; Camalli, M.; Cascarano, G. L.; Giacovazzo, C.; Guagliardi, A.; Moliterni, A. G. G.; Polidori, G. P.; Spagna, R. *J. Appl. Crystallogr.* **1999**, *32*, 115.

SHELXL97.[21] Non-hydrogen atoms were treated anisotropically. Hydrogen atoms were all located by Fourier-methods and refined with isotropic temperature factors and C−H values of 0.93(1) Å. To better evaluate intermolecular contacts, standard neutron C−H distances of 1.08 Å were used.

Chemicals and Reagents. All air- and water-sensitive chemical reactions were performed under dry nitrogen atmosphere. The solvents were reagent grade and were distilled before the use, or dried by conventional methods and distilled under nitrogen.

Benzo[1,2-b;4,3-b′]dithiophene (1a), 2-Methyl(Chlorotriphenyl)phosphine Thiophene (5a), 2-({(2-benzo[1,2-b;4,3-b′]dithiophene)vinyl}thiophene) (6a), 2-({(2-Benzo-[1,2-b;4,3-b′]dithiophene)vinyl}(2-benzo[1,2-b;4,3-b′]-dithiophene) (6b), Trithia[5]heterohelicene (TH5), and Tetrathia[7] heterohelicene (TH7). These compounds were synthesized according to literature methods.[9,13,14]

Benzo[1,2-b;4,3-b′]dithiophene-2-carboxyaldehyde (2a) and Trithia[5]heterohelicene-2-carboxyaldehyde (2b). These compounds were synthesized by dissolving (6.2 mmol) of the appropriate reagent **1a** (or **1b** = **TH5**), $POCl_3$ (8.3 mmol), and *N*-methylformanilide (8.3 mmol) in 4.2 mL of toluene. The magnetically stirred mixture was heated in an oil bath for 3 h for **2a** or 21 h for **2b,** maintaining temperatures between 75 and 95 °C. The hot reaction mixture was poured in a sodium acetate solution, ether or CH_2Cl_2 was added, and the whole mixture was transferred to a separatory funnel. After separation of the organic layer, the aqueous solution was extracted with the appropriate solvent, and the combined organic solution was washed with dilute hydrochloric acid and a sodium bicarbonate solution. After drying over anhydrous Na_2SO_4, the solvent was evaporated and the residue chromatographed over silica gel. Elution with 8/2 hexane/ethyl acetate gave 50% of **2a** and 41% of unreacted **1a**. In the case of **2b** the elution was carried out with 3/7 hexane/CH_2Cl_2 and gave 11% of **2b** and 69% of unreacted **1b.**

Benzo[1,2-b;4,3-b′]dithiophene-2-methyl Alcohol (3a). To a stirred solution of aldehyde **2a** (1.4 mmol) in a mixture of ethanol (1.4 mL) and THF (1.2 mL), 4.1 mmol of sodium borohydride at 0 °C was added. The solution was stirred for 2.5 h at room temperature. Diethyl ether was added and then a saturated aqueous citric acid solution to decompose the remaining sodium borohydride. The reaction mixture was diluted with water and extracted with diethyl ether. The organic phase was dried over Na_2SO_4 and, after solvent elimination, gave **3a** in quantitative yield. The compound was used for the next step without purification.

Trithia[5]heterohelicene-2-methyl Alcohol (3b). To a solution of aldehyde **2b** (0.32 mmol) in a mixture of ethanol (4.88 mL) and THF (3.88 mL) stirred for 30 min, 1.53 mmol of sodium borohydride at 0 °C was added. The solution was stirred for 2.5 h at room temperature. Dichloromethane was added and then saturated aqueous citric acid solution to decompose the remaining sodium borohydride. The reaction mixture was diluted with water and extracted with CH_2Cl_2. The organic phase was dried over Na_2SO_4 and, after solvent elimination, gave **3b** in quantitative yield. The compound was used for the next step without purification.

Benzo[1,2-b;4,3-b′]dithiophene-2-chloromethyl (4a). To a stirred solution of alcohol **3a** (1.6 mmol) in benzene (8.9 mL), pyridine (3.2 mmol) and thionyl chloride (3.2 mmol) at 0 °C under nitrogen were added. The reaction mixture was allowed to warm to room temperature and was stirred overnight. The reaction mixture was then diluted with benzene, the solution was poured into water and was extracted with benzene. The combined organic phases were dried over Na_2SO_4, and, after solvent elimination, gave **4a** in quantitative yield. The compound was used for the next step without purification.

Trithia[5]heterohelicene-2-chloromethyl (4b). To a stirred solution of alcohol **3b** (0.66 mmol) in benzene (6.4 mL), pyridine (1.99 mmol) and thionyl chloride (1.99 mmol) at 0 °C under nitrogen were added. The reaction mixture was allowed to warm to room temperature and was stirred overnight. After 24 h the solution was cooled at 0 °C again, and pyridine (1.99 mmol) and thionyl chloride (1.99 mmol) were added again. The reaction mixture was allowed to warm to 90 °C and was stirred for 4 h. The reaction mixture was then diluted with benzene, and the solution was poured into water and was extracted many times with benzene. The combined organic phases were dried over Na_2SO_4, and, after solvent elimination, gave **4b** in quantitative yield. The compound was used for the next step without purification.

Benzo[1,2-b;4,3-b′]dithiophene-2-methyl Chlorotriphenylphosphine (5b) and Trithia[5]heterohelicene-2-methyl Chlorotriphenylphosphine (5c). A solution of chloride **4a** or **4b** (0.64 mmol) and triphenylphosphine (1.48 mmol) in benzene (9 mL) was heated under reflux overnight. The solid salt was filtrated and washed with benzene to solubilize the remaining triphenylphosphine. The respective yields were 69% for salt **5b** and 27% for salt **5c.** The compounds were used for the next steps without purification.

2-({(2-Benzo[1,2-b;4,3-b′]dithiophene)vinyl}thieno[3,2-e;4,5-e′]bis(benzo[b]thiophene) (6c) and 2-({Thieno[3,2-e;4,5-e′]bis(benzo[b]thiophenyl)vinyl}-Thieno[3,2-e;4,5-e′]bis(benzo[b]thiophene) (6d). The flask was purged with anhydrous nitrogen, and a slow nitrogen stream was maintained during the reaction. To 6 mL of anhydrous methanol, 0.19 mmol of **5b** or **5c** and 0.17 mmol of the aldehyde **2b** were added. The aldehyde, in contrast with the phosphonium salt, did not dissolved completely. The mixture was vigorously stirred, and 0.6 mL of 2.1 M $NaOCH_3$ in methanol was added. The reaction mixture was allowed to reflux for 45 min and cooled; the precipitate was filtered off with suction and washed with water. The yield of the pure product **6c** was 78%. In the case of **6d** purification with column chromatography on silica gel (7/3 hexane/CH_2Cl_2) gave the desired product in 81% yield.

Compound 6c. Yellow solid; mp 163−165 °C. MALDI-mass: $[M]^{\cdot+}$ 510.8. Isotopic ratio: M/M + 2 = 100/27.7. ^{1}HNMR ($CDCl_3$): δ 6.91−8.53 (multiplet). Anal. Calcd for $C_{28}H_{14}S_5$ (%): C, 65.85; H, 2.76; S, 31.39. Found (%): C, 65.91; H, 2.77; S, 31.42.

Compound 6d. Yellow solid; mp 112−115 °C. MALDI mass: $[M]^{\cdot+}$ 616.9. Isotopic ratio: M/M + 2 = 100/34.3. ^{1}HNMR ($CDCl_3$): δ 5.51−7.40 (multiplet). Anal. Calcd for $C_{34}H_{16}S_6$ (%): C, 66.20; H, 2.61; S, 31.19. Found (%): C, 66.37; H, 2.62; S, 31.14.

Pentathia[9]heterohelicene (TH9). A solution of the compound **6c** (0.039 mmol) in 220 mL of benzene, which contained a trace of iodine was irradiated using 16 lamps (350 nm) in a Rayonet reactor. After irradiation for 2 h, the solvent was removed at reduced pressure and the crude product was purified by a column chromatography on silica gel (7/3 hexane/CH_2Cl_2) to give **TH9** in quantitative yield. **TH9** was crystallized from $CHCl_3$ in yellow needles. Melting point > 300° C. ^{1}H NMR signals are reported in Table 2. λ_{max} (ϵ, cm^{-1} mol^{-1}): 293 (12 375), 315 (10 250), 328 (9750), 348 (9500), 401 (9375), 423 (10 500). Anal. Calcd for $C_{28}H_{12}S_5$ (%): C, 66.11; H, 2.38; S, 31.52. Found (%): C, 65.95; H, 2.37; S, 31.54.

Hexathia[11]heterohelicene (TH11). A solution of the compound **6d** (0.039 mmol) in 100 mL of benzene, which contained a trace of iodine, was irradiated using 16 lamps (350 nm) in a Rayonet reactor. After 4 h irradiation, the solvent was removed at reduced pressure and the crude product was purified with a HPLC column chromatography over silica gel (7/3 hexane/CH_2Cl_2) to give **TH11** (60% yield). **TH11** was crystallized with $CHCl_3$ in dark yellow crystals; melting point > 300° C. ^{1}H NMR signals are reported in Table 2. λ_{max} (ϵ, cm^{-1} mol^{-1}): 305 (8500), 355 (6000), 345 (6625), 363 (6750, 380 (9375), 425 (3875), 445 (2500). Anal. Calcd for $C_{34}H_{14}S_6$

(18) Oelkrug, D.; Fegelhaaf, H.−J.; Gierschner, J.; Tompert, A. *Synth. Met.* **1996** *76*, 249.

(19) Becker, R. S.; Seixas de Melo, J.; Maçanita, A.; Elisei, F. *Pure Appl. Chem.* **1995** *67*, 9.

(20) Desiraju, G. R.; Steiner, T. *The Weak Hydrogen Bond*; International Union of Crystallography, Oxford Science Publication: Oxford, U.K., 2000.

(21) Sheldrick, G. M. *SHELXL97*, Release 97−2, Program for the Refinement of Crystal Structures; University of Göttingen: Göttingen, Germany, 1997.

Scheme 1. Pathways for the Synthesis of Thio[*x*]helicenes

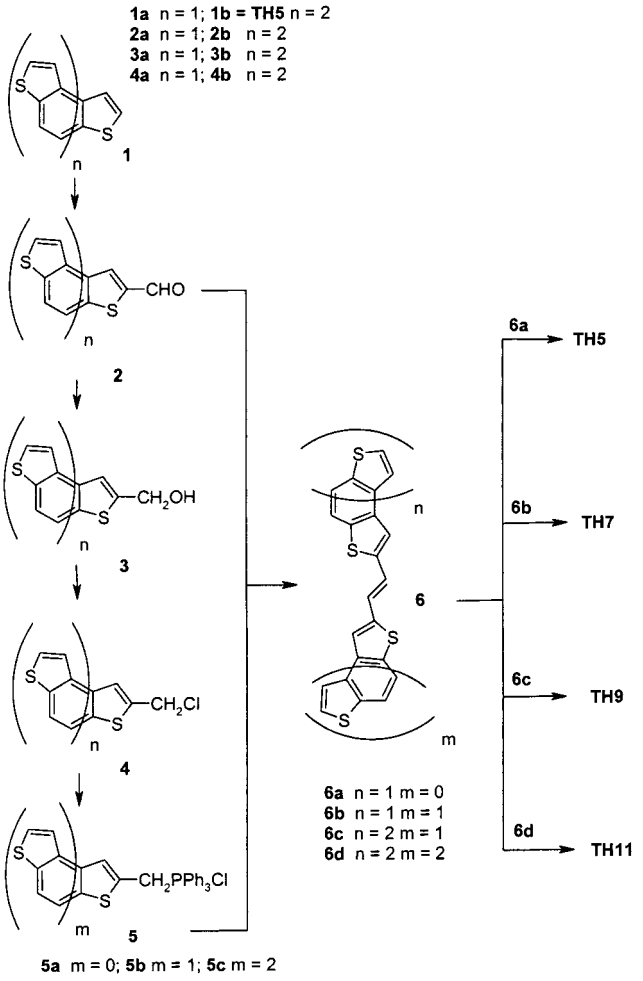

(%): C, 66.42; H, 2.30; S, 31.29. Found (%): C, 66.46; H, 2.29; S, 31.35.

Results and Discussion

Synthesis. The synthesis of thiohelicenes is a laborious process that has a crucial step in the photocyclization of 1,2-diheteroarylethylene.[8] Substituted thiohelicenes may also be obtained in good yield by chemical synthesis both in racemic and in enantiomeric form.[15,16]

We obtained a series of unsubstituted thiohelicenes using a general procedure for the preparation of racemic molecules, shown in Scheme 1, where the photochemical cyclization represents the final step. With this synthetic route it was possible to obtain molecules as large as the 9- and 11-membered thiohelicenes.

Two approaches were, in principle, possible for synthesizing large condensed systems. The first consists of the double photochemical ring closure of a bis(1,2-diheteroaryl)ethylene. In this case the bis-ethylene molecule needs only to contain a heteroaryl moiety that does not exceed three members and can be easily prepared. The second possibility consists of a single photochemical cyclization of a 1,2-diheteroarylethylene, and in this case larger heteroaryl substituents, such as thio[5]heterohelicenes, are necessary. For the synthesis of higher thiohelicenes we preferred the latter approach, to maximize the yield and increase the rate in the critical photochemical step.

Table 1. Energy Required for the Synthesis of Some Helicenes Using Rayonet or Solfin Reactors

product	Rayonet,[a] W h	Solfin,[b] W h
1a	2688	25
TH5	2240	25
TH7	2464	25

[a] Determined using the standard potassium ferrioxalate actinometry. [b] Determined using the energy available typically at noon with the solar spectrum up to 450 nm and aperture area of the collector of 0.2 m^2.

The synthesis of thio[*x*]helicene ($x = 7, 9$ condensed rings) starts by reacting thio[$x - 4$]helicene with Vilsmeier reagent ($POCl_3$ and PhN(Me)CHO in boiling toluene) in order to obtain the corresponding 2-carboxyaldehyde. The phosphonium salt **5** is produced from the 2-carboxyaldehyde **2** with a sequence of reactions illustrated in Scheme 1 and described elsewhere.[14] The Wittig reaction between the phosphonium salt and the 2-carboxyaldehyde of the thio[$x - 4$]helicene gives a 1,2-diheteroarylethylene. The racemic thio[*x*]helicene can be easily obtained with high yield by the photoinduced cyclodehydrogenation of appropriate 1,2-diheteroarylethylenes. The synthesis of the larger esathia[11]helicene **TH11** begins with the reaction between the 2-carboxyaldehyde-thio[5]helicene **2b** and the phosphonium salt of the thio[5]helicene **5c**, followed by photocyclization of the 1,2-diheteroarylethylenes **6a**. As stated above, the synthesis of **1a**, **TH5**, and **TH7** was run either in a Rayonet photoreactor or in a larger scale using the solar light in the "Solfin" reactor. In both cases the chemical yields are the same, but in the Solfin reactor irradiation times are much shorter (generally 2 h). The amounts of energy, required for the conversion of the starting material to the corresponding helicene in the Rayonet reactor and in the Solfin reactor, are reported in Table 1. The energy in watt hours given for the Solfin reactor is the energy available typically at noon (11.00 am to 1.00 pm on a sunny October day, when the solar experiments were performed) with the solar spectrum up to 450 nm and with the aperture area of the collector (0.2 m^2). The striking difference in required energy may, at least in part, be ascribed to the fact that the reactions in the Rayonet reactor are performed under static conditions, while for those in the Solfin reactor, the solution is constantly flowed through the tube placed in the focus of the solar collector.

Mass and NMR Spectra. Laser desorption/ionization time-of-flight mass spectrometry with or without matrix (MALDI-TOF-MS and LDI-TOF-MS, respectively) turned out to be a quick and efficient tool for the determination of the molecular mass of thiohelicenes. Moreover, direct monitoring of the reaction course could be achieved by directly sampling the reaction mixture on the sample slide and acquiring the spectrum in a few minutes. For **TH7** the spectrum shows the molecular ion $M^{\cdot+}$ at *m*/*z* 402.0 and the peak at *m*/*z* 404.2 corresponding to the M + 2 isotope, mainly due to the contribution of ^{34}S. The analysis of the isotopic clusters also provided an efficient way to assess the S content of the final product. For example, the peak intensity ratio M/M + 2 for **TH7** $C_{22}H_{10}S_4$ was 100/21.0, in good agreement with the calculated value 100/20.4 for the same molecular composition. Similar results were obtained for **TH9** and **TH11**, where the peak intensity

Table 2. ^{1}H NMR Assignment of Thia[*x*]heteroelicenes: Multiplicity, Chemical Shift (δ, ppm), Coupling Constants (Hz), Integral (See Chart 1 for Atom Labeling)

	Ha	Hb	Hc	Hd	He	Hf	Hg
1a	d, 7.31, $J = 5.6$, 2H	d, 7.31, $J = 5.6$, 2H	s, 7.42, 2H	–	—		
TH5	dd, 8.15, $J = 5.6$; $J \sim 0.5$, 2H	d, 7.20, $J = 5.6$, 2H	dd, 7.55, $J = 8.5$; $J \sim 0.5$, 2H	d, 7.45, $J = 8.5$; 2H	—		
TH7	dd, 6.78, $J = 5.6$; $J = 0.9$, 2H	d, 6.39, $J = 5.6$, 2H	dd, 7.59, $J = 8.5$; $J = 0.9$, 2H	d, 7.55, $J = 8.5$; 2H	s, 7.53, 2H		
TH9	br d, 5.58, $J = 5.6$; 2H	d, 6.37, $J = 5.6$, 2H	a	a	a	a	
TH11	br d, 5.30, $J = 5.6$; 2H	d, 6.34, $J = 5.6$, 2H	a	a	a	a	s, 7.86, 2H

[a] Not reported as partially overlapped with solvent signals.

Chart 1. Atom Labelling Used in NMR Discussion[a]

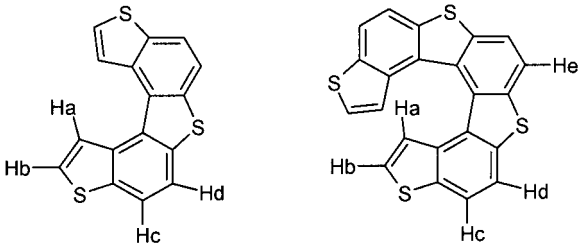

[a] H atoms are labeled in alphabetical order (a–g) starting from H-3 of the terminal thiophene ring. For the sake of clarity only **TH5** and **TH7** are displayed.

ratio M/M + 2 was found to be respectively 100/27.0 and 100/33.9 compared with the calculated values of 100/26.5 and 100/33.4.

The main results of ^{1}H NMR spectra are reported in Table 2. The spin systems occurring within the polithia-[*x*]heteroelicenes can be grouped into two sets including compounds with $x = 3$, 7, 11 and $x = 5$, 9, respectively. The former is characterized by the AB systems of terminal thiophenes, two equivalent H nuclei of the central benzene ring, and one or two other AB systems due to nonterminal benzene rings (one for $x = 7$ and two for $x = 11$). The latter set shows the AB system of terminal thiophenes and one or two AB systems of benzene rings (one for $x = 5$, two for $x = 9$). The symbols used for atom labeling are sketched in Chart 1.

The spectral assignment of protons on thiophene or benzene residues was based on the value of J(orto), 5.6 and 8.5 Hz, respectively. The assignment of protons in positions 2 or 3 with respect to the S atom of thiophene (labeled as Hb and Ha) was supported by the detection of long-range coupling constants between Ha and Hc, due to their zigzag arrangement. The chemical shift of the hydrogen atoms attached to the terminal thiophene rings turned out to be highly sensitive to the molecular helicization. Data in Table 2 show that the observed value for Ha increases dramatically on passing from the reference compound with $x = 3$ to the superior homologue with $x = 5$, consistent with a deshielding of Ha caused by the ring current of the aromatic ring system. Further helicization of the molecular building causes Ha to enter the shielding cone of the aromatic ring systems, thus determining a constant decrease in chemical shift.

Absorption and Emission Properties. The electronic absorption and emission spectra of the thio[*x*]-helicenes in solution are reported in Figure 2. The number of observed transitions in the absorption spectra grows with molecular size, and the transition frequencies, especially at higher energy, evidence the two mentioned thia[*x*]helicene families, namely, the molecules with $x = 5$, 9 characterized by a central thiophene

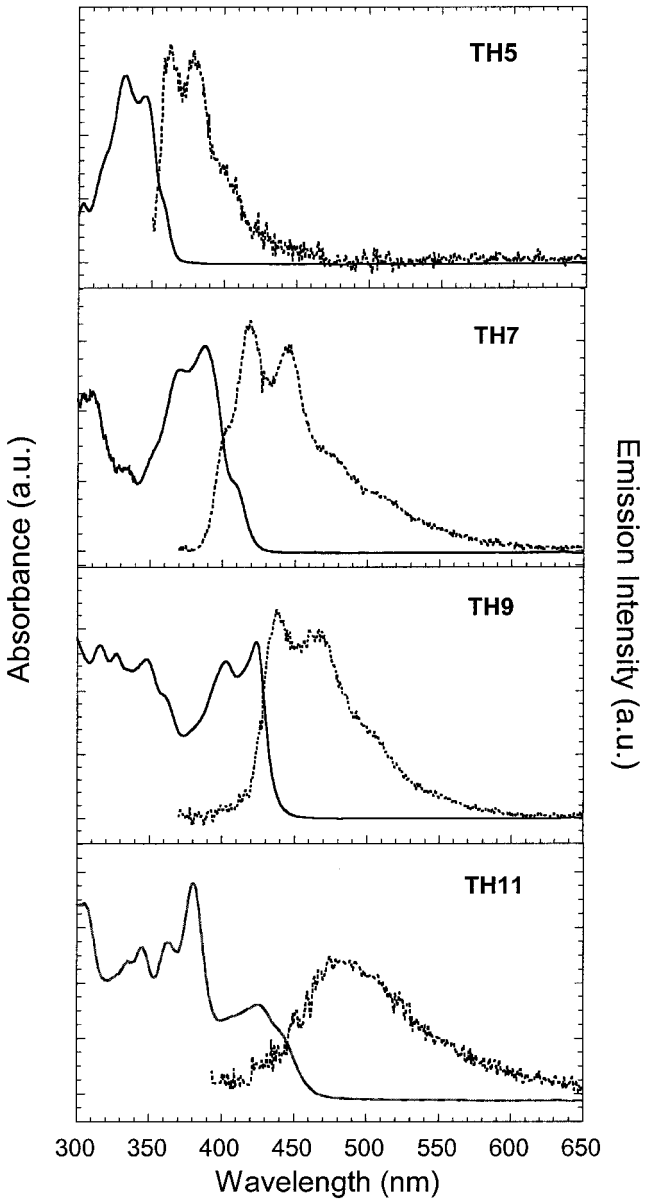

Figure 2. Absorption and emission spectra measured in solution, for the thiohelicene series.

and those with $x = 7$ and 11, having a central benzene. The almost "mirror symmetry" of the lowest energy absorption bands and of the emission spectra helps in identifying the HOMO–LUMO transition which is exhibiting a vibrational progression.

Increasing the number of condensed rings, the absorption bands and the photoluminescence spectra shift to lower energy and there is a reduction of the extinction coefficient and a redistribution of the oscillator strengths from the HOMO–LUMO transition toward the highest energy transitions. This redistribution is particularly

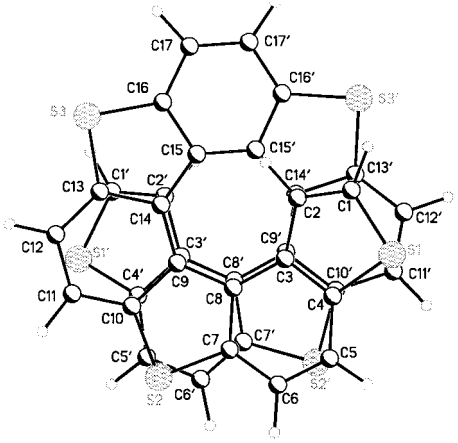

Figure 3. Views of **TH11** down the helix axis

evident for **TH11**. The red shift of the spectra is a consequence of the lengthening of the π-conjugation in the helical system and is a common feature for other conjugated molecules. However the observed changes of the oscillator strengths with the molecular size have an opposite behavior with respect to linear thiophene- or phenylene-based oligomers. Contrarily to thiohelicenes, these classes of molecules exhibit an increase of the HOMO−LUMO oscillator strength increasing the molecular size.[18]The emission quantum yields are respectively 1.64×10^{-2} (**TH5**), 4.53×10^{-2} (**TH7**), 4.42×10^{-2} (**TH9**), and 1.2×10^{-2} (**TH11).** The changes of the efficiency with the molecular size are consistent with the variation of the extinction coefficients. The quantum yields are low for the whole thiohelicene series, thus evidencing that efficient nonradiative decay is occurring. The presence of the sulfur atoms suggests that nonradiative decay may be due to intersystem crossing to the triplet manifold. Since phosphorescence has not been detected, there is not direct evidence for this disexcitation pathway, but similarly to oligothiophenes, nonradiative decay of the triplet state by thermal motion may possibly occur.[19] The changes of the optical properties just described allow some rationalization in terms of increasing intramolecular interactions between π-electron systems of overlapping rings in large helicenes.

Molecular Structure and Packing. Figures 3 and 4 respectively show the molecular structure and the packing of the eleven-membered helicene **TH11** as obtained by single-crystal X-ray diffraction. Although preliminary data on the crystal structure of the nine-membered system have already been reported,[9] we will discuss them in more detail here. Figures 5 and 6 show views of the molecular structure and of the packing of **TH9**, while essential features of the molecular geometry of the two compounds are given in Tables 3−5, along with literature data for the thia[*x*]helicene family, namely, the molecules with $x = 5,7$,[11,12] i.e., the only two other racemic thiohelicenes available. It should be noted that all the thiohelicenes we discuss have a C_2 molecular symmetry, the 2-fold axis bisecting the central ring in the molecules. Since in the molecules both terminal rings are thiophenes, numbering will proceed from terminal rings for homogeneity and atoms related by the 2-fold intramolecular axis will carry the same label but be primed.

Both **TH9** and **TH11** show evidence of increased twisting as compared to lower racemic oligomers: they

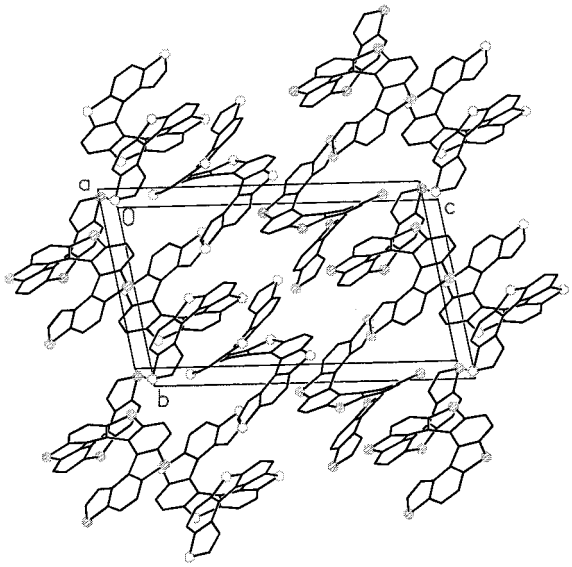

Figure 4. Packing of **TH11** along the *b* axis of the unit cell. The two nonequivalent molecules are clearly apparent.

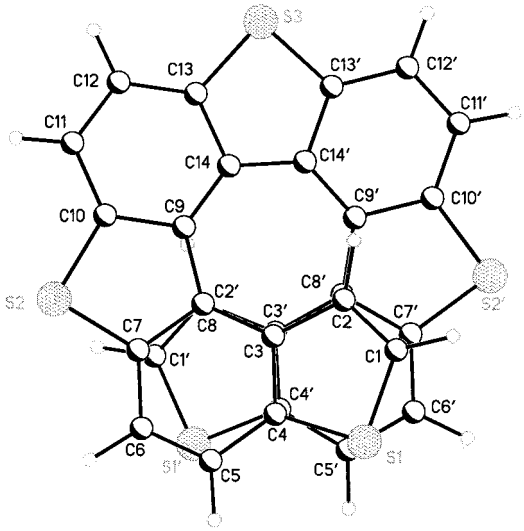

Figure 5. Views of **TH9** down the helix axis.

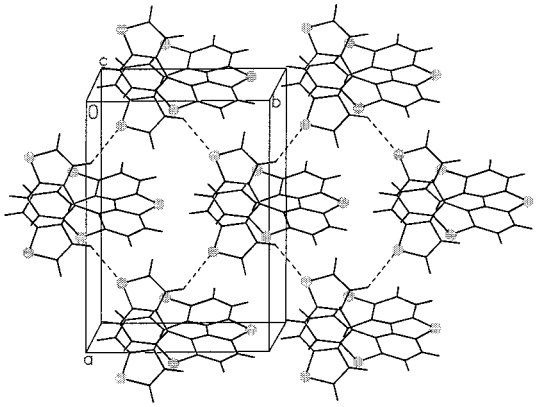

Figure 6. Isochiral molecules planes, parallel to the *ab* lattice plane, alternating in **TH9** crystals.

are the first studied thiohelicenes for which more than one helical turn is completed. The idealized infinite helices (built by C_6H_2S repeats, i.e., one thiophene ring plus two additional carbons of the sequential phenyl) approach closely a 7_2 symmetry. This is apparent in Figures 3 and 5, showing the two molecules in views

Table 3. Selected Geometrical Features of Thio[*x*]helicenes (Estimated Standard Errors in Parentheses)[a]

	TH11(1)	TH11(1′)	TH11(2)	TH11(2′)	TH9	TH7[b]	TH5[c]
			Bond Lengths (Å)				
C2−C3$^{(ti)}$	1.432(8)	1.441(8)	1.439(8)	1.442(8)	1.436(3)	1.429(6)	1.435(3)
C3−C8$^{(bi)}$	1.433(8)	1.429(7)	1.428(7)	1.406(8)	1.423(3)	1.426(5)	1.423(3)
C8−C8′$^{(ti)}$							1.456(3)
C8−C9$^{(ti)}$	1.470(7)	1.436(7)	1.456(7)	1.455(7)	1.449(3)	1.454(6)	
C9−C9′$^{(bi)}$						1.443(6)	
C9−C14$^{(bi)}$	1.431(8)	1.432(8)	1.419(7)	1.427(7)	1.421(3)		
C14−C15$^{(ti)}$	1.455(8)	1.433(7)	1.446(7)	1.452(7)	1.451(4)		
C15−C15′$^{(bi)}$	1.418(7)	1.418(7)	1.425(7)	1.425(7)			
C5−C6$^{(be)}$	1.353(9)	1.378(8)	1.364(9)	1.362(9)	1.371(4)	1.376(7)	1.360(5)
C11−C11′$^{(be)}$						1.356(7)	
C11−C12$^{(be)}$	1.387(9)	1.371(10)	1.364(9)	1.356(9)	1.361(4)		
C17−C17′$^{(be)}$	1.346(9)	1.346(9)	1.372(9)	1.372(9)			
			Bond Angles, q (°)				
C2−C3−C8	132.3(5)	130.6(5)	130.9(5)	130.8(5)	130.1(2)	130.3(4)	130.9(3)
C3−C8−C8′							131.3(2)
C3−C8−C9	130.7(5)	131.0(5)	131.0(5)	131.9(5)	130.8(2)	131.4(4)	
C8−C9−C9′						133.0(4)	
C8−C9−C14	132.0(5)	132.0(5)	132.2(5)	131.9(5)	132.2(2)		
C9−C14−C15	131.7(5)	131.7(5)	131.8(5)	132.3(5)	132.4(1)		
C14−C15−C15′	131.5(5)	131.3(5)	132.1(5)	132.6(5)			
			Torsion Angles, j (°)				
C2−C3−C8−C8′$^{(bi)}$							11.3(4)
C2−C3−C8−C9$^{(bi)}$	5.5(11)	6.2(10)	4.7(10)	4.8(11)	10.0(4)	5.1(8)	
C3−C8−C8′−C3′$^{(ti)}$							20.5(4)
C3−C8−C9−C9′$^{(ti)}$						16.4(8)	
C3−C8−C9−C14$^{(ti)}$	17.9(10)	18.8(10)	17.8(10)	16.6(10)	21.7(4)		
C8−C9−C9′−C8′$^{(bi)}$						23.2(8)	
C8−C9−C14−C15$^{(bi)}$	17.9(10)	18.6(10)	21.2(10)	19.4(10)	15.6(4)		
C9−C14−C15−C15′$^{(ti)}$	21.5(10)	22.2(10)	20.3(10)	20.4(10)	15.7(4)		
C14−C15−C15′−C14′$^{(bi)}$	12.1(10)	12.1(10)	11.6(10)	11.6(10)			
			Ring Root Mean Square D[d] (Å)				
A	0.019	0.010	0.011	0.016	0.015	0.013	0.012
B	0.035	0.033	0.028	0.033	0.044	0.030	0.057
C	0.042	0.037	0.048	0.040	0.047	0.035	0.045
D	0.062	0.061	0.062	0.060	0.065	0.035	
E	0.056	0.056	0.052	0.054	0.048		
F	0.076	0.076	0.073	0.073			
			Interring Angle,[e] π (deg)				
AB	7.6(4)	10.6(3)	8.7(4)	8.7(4)	9.7(1)	8.8(2)	10.6(1)
BC	8.7(4)	9.9(3)	10.7(4)	9.6(3)	9.6(1)	8.6(1)	7.9(2)
CD	9.9(3)	9.2(3)	11.3(3)	11.4(3)	10.5(1)	11.3(1)	
DE	10.5(3)	10.8(2)	9.8(2)	9.6(2)	9.2(1)		
EF	10.6(2)	11.1(2)	10.8(2)	9.8(2)			

[a] The labels (1), (1′), (2), and (2′) for **TH11** refer to the two independent molecules (1 and 2) in the crystal structure and the two halves of the two molecules interrelated by noncrystallographic 2-fold axes (see Chart 2 and Figure 3). [b] Adapted from ref 12, using the atom labeling (Chart 1) adopted for **TH11** and **TH9**, and priming atoms related by a 2-fold axis bisecting the central ring of the reference asymmetric unit. [c] Adapted from ref 11; labeling as for footnote *b*. [d] Root-mean-square atom deviations **Δ** from ring least-squares planes. See Chart 1 for ring labeling. [e] Dihedral angles between contiguous ring least-squares planes in **TH11**, **TH9**, **TH7,** and **TH5:** $^{(ti)}$ thiophene bond lengths, or torsion angles centered on a thiophene bond, at the helix interior; $^{(bi)}$ benzene bond lengths, or torsion angles centered on a benzene bond, at the helix interior; $^{(be)}$ benzene bond lengths at the helix exterior.

down the helical axis, as the terminal thiophene rings closely superimpose with the eighth ring (a benzene), yielding half the periodicity of an infinite helix. Least-squares planes of rings separated by six other rings are nearly parallel. Projection superposition between two thiophene rings, attaining the helical periodicity will roughly occur after 2 turns and 14 rings, i.e., after 7 C_6H_2S units. The pitch of the helices increases slightly with molecular size ranging from ca. 3.0 Å to 3.1 and 3.2 Å in thia[*x*]helicenes respectively with $x = 7$, 9, and 11**.** Short intramolecular contacts occur between atoms close to the helix axis and seven rings apart (Table 4); in **TH7** there are only three of these contacts, while a number of different contacts of this kind occur in **TH9** and in each the two independent molecules of **TH11**. The shorter intramolecular contacts of this kind, 0.3 Å or more below the sum of van der Waals radii, must be repulsive: they arise because of the tendency inherent in polyconjugated systems to deviate as little as possible from planarity. Deviations from planarity are clearly more concentrated in central rings, whereas terminal rings are more nearly planar as apparent from the data in Table 3. Informative parameters with respect to steric interactions are the dihedral angles π between the least-squares planes of adjacent rings (see Chart 2 for ring nomenclature), the bond angles θ at the benzene−thiophene junction close to the helix axis, and the torsion angle φ on the C−C bonds at the interior of the helices (see Figures 3 and 5 and Table 3). The average values of all these parameters (Table 5) tend to increase from **TH5** to **TH11**. However, if we separate the contributions to the averages of the terminal from those of the internal rings, we can see that the increase is mainly determined by the larger number of internal rings, as the molecular size grows, rather than by individually larger contributing figures. Close to as-

Table 4. Short Intramolecular Contacts[a] in TH11, TH9, TH7, and TH5

contact (Å)	TH11(1)	TH11(2)	TH9	TH7[b]	TH5[c]
C2···C14′	3.115	3.214			
C2···C15′	3.018	3.072			
C2···C15	3.293	3.288			
C3··C14′	3.166	3.255			
C8···C9′	3.129	3.175			
C9···C3′	–	3.283			
C9···C8′	3.140	3.161			
C14···C2′	3.207	3.097			
C14···C3′	3.198	3.219			
C15···C2′	3.041	3.016			
C2···C15′	3.265	3.275			
C2···C8′			3.084		
C2···C9′			3.032		
C3···C3′			3.174		
C3···C8′			3.085		
C8···C2′			3.084		
C8···C3′			3.085		
C9···C2′			3.032		
C2···C2′				3.012	
C2···C3′				3.116	
C3···C2′				3.116	
C2···C2′					3.231

[a] C···C contacts below 3.30 Å. No S···C contacts below 3.80 Å are found. The labels (1) and (2) for **TH11** refer to the two independent molecules in the crystal structure. [b] Adapted from ref 12, using the atom labeling adopted for **TH11** and **TH9**, and priming atoms related by a 2-fold axis bisecting the central ring the reference asymmetric unit. [c] Adapted from ref 11; labeling as for footnote *b*.

Table 5. Average Structural Parameters in Racemic Thiahelicenes

param	TH5[a]	TH7[b]	TH9	TH11
ρ^c (Mg m^{-3})	1.570	1.576(1.526 [d])	1.573	1.581
π^e (deg)	9.2	9.6(8.90 [d])	9.8	10.0
θ^f (deg)	131.1	131.6	131.4	131.6
φ^g (deg)	14.4	13.2	15.8	15.4
$CC_{av\ thioph\ int}$ (Å)	1.442	1.441	1.444	1.446
$CC_{av\ benz\ int}$ (Å)	1.423	1.432	1.422	1.425
$CC_{av\ benz\ ext}$ (Å)	1.360	1.368	1.366	1.365

[a] Adapted from ref 11. [b] Adapted from ref 12. [c] ρ is the density. [d] Refers to the **TH7** pure enantiomer crystal structure. [e] π is the average dihedral angle between least-squares planes of contiguous rings. [f] θ is the average bond angle at the helix interior. [g] φ is the average torsion angle at the helix interior.

ymptotic values appear to be attained already with **TH7**. The torsion angle values, and especially the terminal torsion angle φ (see Table 3), reflect the existence of the two distinct subgroups in thia[*x*]-helicenes: (i) systems with $x = 5$ and 9 having a thiophene as central ring and (ii) molecules with $x = 7$ and 11 with a central benzene. Similar conclusions can also be reached by considering the sequences of dihedral angles π between adjacent least-squares ring planes and the root mean square deviations Δ from the planes in Table 3. As reported in the case of carbohelicenes[22−28]

Chart 2. Ring Labeling in TH11[a]

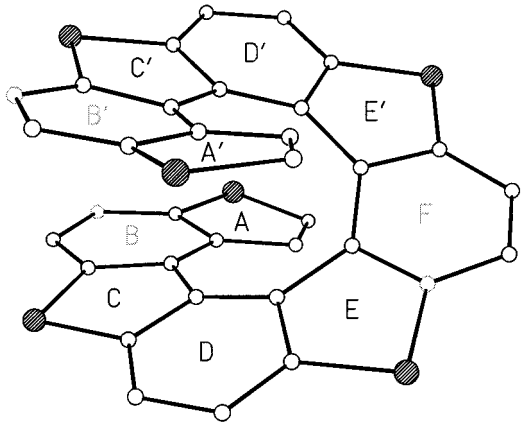

[a] A similar labeling, starting from the terminal rings, is adopted for the other molecules. Rings related by the C_2 axis bisecting the central ring are primed. Note that this symmetry element is rigorous for **TH5**, **TH7**, and **TH9**, but noncrystallographic in the case of **TH11**.

and for lower thiohelicenes,[11,12] because of steric strain, the benzene carbon−carbon bond lengths at the helix interior are substantially longer than at the periphery. In this respect the values found in both the larger thiahelicenes closely match those already reported for **TH5** and **TH7**. Bond length distortions (Table 3) appear on the other hand smaller than those of carbohelicenes. Consistent with a less strained structure, values of φ, but also of π, are significantly smaller in thiohelicenes than in carbohelicenes. Average values close to 10 and 16° for π and φ, respectively, in both **TH9** and **TH11** (Table 5), compare with 12.5 and 23.7° in the 10-ring carbohelicene.[24] Accordingly also intramolecular contacts are less severe, irrespective of the presence of the somewhat bulkier S atom (Table 4). This is due to the alternation of five- and six-membered rings which reduces atomic overlap and requires 7 as opposed to 6 rings to complete a helical turn, spreading distortions on a larger number of rings and widening the helix diameter by ∼0.7 Å, i.e., ca. 6%.

In racemic thiohelicenes, including **TH9** and **TH11**, the aggregation of antipodes is apparent: it occurs by $\pi-\pi$ stacking in highly interdigitated columnar architectures. While all the available thiohelicene structures show rows of isochiral molecules, interactions among them are generally looser than for enantiomers and they are normally mediated by molecules of opposite chirality. The stacking occurs between specific molecular sections of enantiomeric pairs: depending upon the particular system, the third and/or the fourth rings from the molecular ends appear to be involved. In all thiohelicene crystals (see Table 6) specific interactions were found involving sulfur[11,12] and hydrogen atoms at distances slightly shorter than the sum of van der Waals radii (1.80 Å for S and 1.20 Å for H). They are quite probably attractive, and, in all structures except **TH11**, they involve only atoms of terminal rings. In the case of the 5-ring system each molecule has two equivalent S···S interactions of 3.544 Å, while each **TH7** molecule is involved in four equivalent S···H contacts measuring 2.89 Å. All these interactions occur between enantiomeric pairs. For **TH9**, each molecule presents four equivalent S···H contacts at 2.87 Å, all with homochiral

(22) Kurota, R. *J. Chem. Soc., Perkin Trans. 2* **1982**, 789.
(23) Van den Hark, T. E. M.; Beurskens, P. T. *Cryst. Struct. Commun.* **1976**, *4*, 247.
(24) Le Bas, G.; Navaza, A.; Mauguen, Y.; de Rango C. *Cryst. Struct. Commun.* **1976**, *5*, 357.
(25) Le Bas, G.; Navaza, A.; Knossow, M.; de Rango C. *Cryst. Struct. Commun.* **1976**, *5*, 713.
(26) Beurskens, P. T.; Beurskens, G.; Van den Hark, T. E. M. *Cryst. Struct. Commun.* **1976**, *5*, 241.
(27) de Rango, C.; Tsoucaris, G. *Cryst. Struct. Commun.* **1972**, *2*, 189.
(28) Le Bas, G.; Tsoucaris, G.; Navaza, A.; Mauguen, Y.; de Rango, C. *Cryst. Struct. Commun.* **1976**, *4*, 237.

Table 6. Intermolecular Interaction Geometries in the Racemic Thiohelicene Series[a]

	C···S (Å)	S···H (Å)	CH···S (°)	sym
TH11				
C1(1)−H1(1)···S1(2)*	3.812	2.94	137.5	$x-1, y, z$
C5(1)−H5(1)···S3′(2)*	3.806	2.89	142.8	x, y, z
C5'(2)−H5′(2)···S3′(1)*	3.809	2.80	156.1	$-x+1, -y, -z+1$
C6(1)−H6(1)···S2(1)*	3.667	2.95	124.3	$-x+1, -y+1, -z$
TH9				
C2−H2···S1*	3.699	2.87	138.3	$0.5+x, 0.5+y, z$
TH7[b]				
C1−H1···S1*	3.743	2.89	140.8	$-x, -y-1, -z-1$
TH11				
	$S_A···S_B$ (Å)	α_A(°)[a]	α_B(°)[b]	sym
S2(1)···S2(1)*	3.398	127.8	127.8	$1-x, 1-y, -z$
S1′(1) ··· S3(1)*	3.424	106.5	130.1	$-x, 2-y, -z$
S1′(1) ··· S3′(2)*	3.582	112.1	109.9	$1-x, 1-y, -z$
S1′(2) ··· S3(2)*	3.562	100.4	132.2	$1-x, 1-y, -z$
TH5[e]				
S1···S1′*	3.544	95.5	95.5	$-x, -y, -z$

[a] Starred atoms are part of a molecule related to the reference molecule by the indicated symmetry operation. Numbers in parentheses in the case of **TH11** specify to which of the independent molecules a given atom belongs. Primed atoms are symmetry related by the intramolecular C_2 axis to unprimed atoms. [b] Adapted from ref 12. [c] Angle between line $S_A···S_B$ and the normal to thiophene ring to which S_A belongs. [d] Angle between line $S_A···S_B$ and the normal to thiophene ring to which S_B belongs. [e] Adapted from ref 11.

molecules giving rise to a quasi-hexagonal packing of tilted helices in planes parallel to the *ab* lattice plane. The crystal structure of **TH11** is unusual because the asymmetric unit is formed by two complete molecules (i.e., molecules 1 and 2), as opposed to half a molecule in all the lower racemic thiohelicenes. The packing environment of each of the two closely similar but crystallographically independent molecules, and of each of its halves, is unique: thus the C_2 axes bisecting the central ring of each **TH11** molecule are noncrystallographic. This situation is likely to arise in order to optimize the complex network of specific interactions involving S and H atoms. It leads to larger than expected asymmetric units and lower crystal symmetry, common occurrences in hydrogen bonded molecular systems. In the triclinic **TH11** crystals four nonequivalent short S···S and an equal number of S···H interactions are found. The essential geometric features of all these contacts in the racemic thiohelicene series are summarized in Table 6, evidencing a remarkable consistency of the S···H interaction with expectations for weak hydrogen bonds.[20] The complex network of specific interactions involving sulfur and hydrogen atoms, generally of terminal rings, probably plays a role determining the surprising near constancy of the density (less than 1% variations, see Table 4) in racemic thiahelicene crystals. On the contrary the density of the racemic seven ring thiohelicene exceeds by 3% that of the chiral **TH7** crystal. Note that in the case of carbohelicenes crystals the density of the eleven ring system is 7% larger than that of the five ring molecule. Also for larger oligomers of the thiohelicene series, homochiral interactions may occur but, at variance with carbohelicenes, heterochiral aggregation is rather consistently more favorable. Specific interactions involving especially terminal ring sulfur and hydrogen atoms up to **TH9**, but also central ring atoms in **TH11**, clearly play a predominant role in the self-assembly pattern favoring heterochiral aggregation and contribute to the determination of hardly predictable, low-symmetry patterns.

Conclusions

A general photochemical synthesis of large thiohelicenes containing 9 and 11 rings has been discussed. The proposed pathway allows the synthesis either in laboratory or in large scale using the solar reactor. The absorption and emission spectral features are consistent with the lengthening of the π-conjugation in helical systems increasing the molecular size. The observed differences with respect to linear polythiophenes may be due to the growing importance of intramolecular interactions between π-electron systems of overlapping rings in large helicenes. MALDI-TOF or LDI-TOF mass spectra turned out to be a convenient technique for the analysis of both the crude reaction mixture and the final purified product. The S content could be assessed by the analysis of the $^{32}S/^{34}S$ isotopic cluster of the molecular ion. ^1H NMR spectra showed that hydrogen atoms in the α position with respect to the S atom of terminal thiophene rings are sensitive probes for the molecular helicity. Electronic spectroscopy, NMR spectroscopy, and X-ray diffraction reveal structural features which are specific for the two families of thiahelicene having respectively a thiophene or a benzene as the central ring The conformation and the crystal architecture of racemic thiohelicenes, containing up to 11 rings, have been examined in detail, revealing ring distortions smaller than in carbohelicenes. All the crystals obtained from racemic products are racemates, whereas for the 10- and 11-ring carbohelicenes chiral crystals are obtained. Heterochiral assembling is dominant also for the larger systems including the 9-ring system, where the specific interactions involving terminal ring S atoms, however, favor the segregation in planes of close-packed homochiral molecules. Asymptotic values are not obtained for various intramolecular properties up to **TH11**; it must be emphasized that end groups still play a major role not only in the packing. Indeed the helix diameter, measuring roughly 12 Å, is still clearly larger than the axial dimension, which, even in the 11-ring system, is still below 10 Å.

Specific interactions, the lower ring distortions and the somewhat larger helix diameter, allow some rationalization of the different self-assembly propensities as compared to carbohelicenes. The interactions involving sulfur atoms may also offer the possibility of even finer modulation of crystalline organization using e.g. thiahelicene building blocks with other molecules in cocrystals.

Supporting Information Available: Tables of crystallographic data and structure factors (PDF). This material is available free of charge via the Internet at http://pubs.acs.org.

CM010093Z